Chaos, Solitons & Fractals xxx (2013) xxx–xxx

Contents lists available at SciVerse ScienceDirect

Chaos, Solitons & Fractals

Nonlinear Science, and Nonequilibrium and Complex Phenomena

journal homepage: www.elsevier.com/locate/chaos

Network of echoes

B.J. West [a], M. Turalska [b,*]

[a] Information Sciences Directorate, US Army Research Office, Research Triangle Park, NC 27709, United States
[b] Department of Physics, Duke University, Durham, NC 25501, United States

ARTICLE INFO

Article history:
Available online xxxx

ABSTRACT

The decision making model (DMM) previously developed [3,35] has been shown to generate phase transitions, to be topologically complex as manifest by inverse power-law (IPL) degree distributions, and to produce temporal complexity through IPL distributions in the switching times between the two critical states of consensus. These properties are entailed by the fundamental assumption that the network elements in the DMM imperfectly imitate one another, which is postulated herein as the echo response hypothesis; an echo being an imperfect copy of an original signal. Some implications of this hypothesis for the human sciences are explored.

1. Introduction

At the turn of the twentieth century a widely accepted theory in social psychology was the Theory of Imitation. Ellwood [12] explained that this theory had two origins; one from the side of the individual and the other from the side of society. Tarde [34] argued that imitation was the fundamental mechanism by which the phenomena of crowds, fads, fashions and crime, as well as other collective behaviors, could be understood, but no mathematical demonstration was provided. On the other side, Baldwin [1] maintained that imitation theory developed out of the mental development of the child resulting from imitation being a basic form of learning. It was believed that because society was a functional combination of individuals all the properties of society were already contained within the individual waiting to be discovered. Imitation theory was a remarkably rigid application of the principle of reductionism and the critique of the theory by Ellwood was firmly anchored in the reductionist tradition.

Ellwood pointed out that imitation theory separated humans from other animals based on their instinct to imitate dominating the entire process of social organization. However he emphasized that this separation was contradicted by data as indicated by herds of elephants, colonies of ants, and swarms of all kinds. The question then arises whether the separation made by the original investigators was inconsistent with the notion of imitation, or was it a consequence of the limitations of verbal as opposed to mathematical reasoning?

Imitation remains an important concept in the human sciences with application inside and outside the social domain. The nascent discipline of neuroscience was developing at the same time that the theory of imitation was being criticized and investigators were associating various physical locations in the human brain with psychological and behavior function. Liepmann [22] determined that human beings are capable of imitating sounds, movements, gestures, etc., and that this ability was lost in patients with lesions in certain areas of the brain. Nearly a century later functional magnetic resonance imaging (fMRI) experiments demonstrated that the same network of cortical regions is activated during a given action, regardless of how that action is initiated [18]. This provided a direct neurological evidence for how the imitation mechanism is realized by the brain.

A significant omission from the early discussions of imitation in the social and neural realms is the fact that no copy is perfect. Nothing is ever done exactly the same way twice, so every copy contains deviations from the original, that is, they contain errors. Physical 'imitators' are

* Corresponding author.
E-mail address: mat51@phy.duke.edu (M. Turalska).

0960-0779/$ - see front matter © 2013 Elsevier Ltd. All rights reserved.
http://dx.doi.org/10.1016/j.chaos.2013.06.005

mirrors and echoes; the former are formed by reflected light and the latter by reflected sound. The accumulated distortion in the reflection process measured at the receiver is determined by a stochastic function and is referred to as noise. The mathematician Norbert Wiener [39] determined that time series could be filtered to remove the noise, which works well for linear processes such as wave reflection but such linearity is rare in the human sciences. Consequently, the additive signal plus noise modeling of echoes is not adequate for understanding the dynamics of imitation in social and cognitive phenomena. The failure of the signal plus noise paradigm is due in large part to imitators in the human sciences being active not passive responders.

The intent here is not to model imitation, nor to present a theory of imitation. Rather imitation is adopted as a basic social/psychological mechanism that is part of what it means to be human. Herein we adopt the hypothesis that imperfect imitation (echo response) is a fundamental mode of human behavior and implement the hypothesis in a mathematical model of networked decision making. The resulting dynamics are then used to determine what the echo response hypothesis (ERH) entails about behavior that is not implicit in the initial statement of the model, and to determine if that behavior corresponds to the kind of cooperation observed in nature.

Using a previously developed decision making model (DMM) [3,35] we establish that the ERH entails criticality and phase transitions that were emphasized in Gerhard Werner's last publication and which he stressed with equal vigor in our last conversations. He was convinced that criticality is fundamental to the understanding of cognition and cooperative behavior, as are we. This cooperation is the very behavior that Ellwood believed the theory of imitation could not explain.

In Section 2 we briefly review the DMM developed and explored by Turalska et al. [35–37] in the study of social interactions. What is new here is the explicit recognition of the importance of the ERH in the formulation of the model and what that entails about criticality in the social domain. Section 2.1 focuses on the properties of the DMM when all the elements in the network are coupled to one another (all-to-all (ATA) coupling) and establishes the existence of a phase transition at a critical value of the control parameter. Section 2.2 extends this analysis to a two-dimensional lattice with nearest neighbor interactions. These local interactions also give rise to a phase transition at a critical value of the control parameter that is larger than in the ATA coupling case. The lattice dynamics are shown to produce inhomogeneous opinion distributions analogous to that observed in the distribution of magnetization on a spin lattice.

The kinds of complexity entailed by the ERH in the DMM are determined in Section 3 to be inverse power laws in the degree distribution as well as in the distribution of times between changing network decisions. As we mentioned it is not only society that is strongly influenced, if not dominated, by collective behavior. Coordinated behavior of the aggregate is also found in the dynamics of real neural networks. The neuronal avalanches produced by criticality in the human brain [2,13] have been described by the DMM as we discuss in Section 4 and in this context the ERH is argued to be a consequence of the recently observed mirror neurons.

In Section 5 we draw some conclusions.

2. Decision making model

There are a number of ways to model complex dynamic networks even restricting the analysis to those in which the ERH can be implemented. One way would be through stochastic differential equations, where the statistical uncertainty in the network dynamics is explicitly modeled by a random force included in the equations of motion. Another is to replace the network dynamics at the level of the individual element with the macroscopic behavior of the probability or population density and follow its evolution in the network's phase space. Herein we model the dynamics of the probability for an individual labeled by α to be in either of the two states $|1\rangle$or $|2\rangle$ by the coupled two-state master equation, which was introduced into physics to describe the evolution of the discrete probability of a stochastic process:

$$\frac{d}{dt}p_1^{(\alpha)} = -g_{12}^{(\alpha)}p_1^{(\alpha)} + g_{21}^{(\alpha)}p_2^{(\alpha)}, \tag{1}$$

$$\frac{d}{dt}p_2^{(\alpha)} = -g_{21}^{(\alpha)}p_2^{(\alpha)} + g_{12}^{(\alpha)}p_1^{(\alpha)}. \tag{2}$$

The quantity $p_j^{(\alpha)}(t)$ is the probability of the element α being in the state $|j\rangle$ with $j = 1,2$ at time t and the probability is normalized at each point in time such that

$$p_1^{(\alpha)} + p_2^{(\alpha)} = 1. \tag{3}$$

The states $|1\rangle$ and $|2\rangle$ correspond to the values +1 and -1, the decision yes or no, or a switch being on or off, etc. The dynamics are determined by the choice of the functional form of the transition rates, that is, the $g's$ in the master equation.

Each node of the network is occupied by a dynamic element whose changes in time are described by the master equation given by the coupled equations, Eqs. (1) and (2). Any individual element is influenced by all the other elements to which it is directly connected according to the prescription for the transition rates in the decision making model (DMM)

$$g_{ij}^{(\alpha)}(t) = g_0 exp\left[K\left\{\pi_j^{(\alpha)}(t) - \pi_i^{(\alpha)}(t)\right\}\right]; \quad i \neq j = 1,2 \tag{4}$$

where

$$\pi_s^{(\alpha)}(t) = \frac{M_s^{(\alpha)}(t)}{M^{(\alpha)}}. \tag{5}$$

$M^{(\alpha)}$ denotes the number of links connected to the element that we are considering and $M_s^{(\alpha)}(t)$ is the number of nearest neighbor elements that are in the state $s = 1,2$ at time t. The parameter K is the control parameter that determines the strength of the interactions between elements of the network and element α. A single element retains its decision in the presence of interactions for a time longer or shorter than $\tau_D = 1/2g_0$ according to the choices made by its neighbors. This is where the echo hypothesis enters our understanding of individual behavior. The single

Please cite this article in press as: West BJ, Turalska M. Network of echoes. Chaos, Solitons & Fractals (2013), http://dx.doi.org/10.1016/j.chaos.2013.06.005

element imitates however imperfectly the majority opinion of those with whom it is connected.

If an element is in the state $|1\rangle$ and half of its neighbors are in the state $|2\rangle$ and half in the state $|1\rangle$, the single element remains in the state $|1\rangle$ as it would in isolation. If the majority of its neighbors are already in the state $|2\rangle$ the single element makes its decision of selecting $|2\rangle$ earlier than it would have in isolation. In the opposite case when the majority of its neighbors are in the state $|1\rangle$ the single element retains its original decision for a longer time than it would in isolation. The ERH therefore has a subtle effect on the dynamics behavior of the individual's decision making. It does not change the individual's statistical behavior instead it modifies the time scale for making decisions.

The key point is that the master equation for each element is well defined, but it is a stochastic master equation, which is to say, the individual probabilities are themselves random functions. In fact the transition coefficients $g_{ij}^{(\alpha)}$ depends on the quantities $\pi_s^{(\alpha)}$, which have random values depending on the stochastic time evolution of the network elements coupled to the element α. Thus we may define another frequency

$$\Sigma_s(t) = \frac{N_s(t)}{N}, \tag{6}$$

where N denotes the total number of elements in the network and $N_s(t)$ the number of those elements in $s = \pm 1$ at time t. It is evident that the quantity Σ_s is also an erratic function of time, even if it is expected to be smoother than π_s. In fact, Σ_s is a global property, obtained from the observation of the entire network, while $\pi_s^{(\alpha)}$ is a property of the immediate environment of a given element α. The smaller the cluster, the more erratic the quantity $\pi_s^{(\alpha)}$. We also define the stochastic global variable

$$\xi(t) \equiv \Sigma_1(t) - \Sigma_2(t) = \frac{N_1(t) - N_2(t)}{N}, \tag{7}$$

whose variability is characteristic of the entire network of echoes, that is, the echoing response of an element to the echoed opinions of its coupling partners.

2.1. All-to-All DMM

In the situation where the number of nearest neighbors coupled to the element of interest consists of all the other individuals in the network we have all-to-all (ATA) coupling; an assumption that is often seen in social theories. Consider the ATA coupling case and assume that the total number of elements within the network N becomes infinite. In the $N \to \infty$ case the fluctuation frequencies collapse into probabilities according to the law of large numbers $\pi_s^{(\alpha)} = \Sigma_s = p_s^{(\alpha)}$ and we can suppress the individual element index. In physics this replacement goes by the name of the *mean field approximation* in which case the transition rates in the master equation for the entire network are written

$$g_{ij} = g_0 exp[-K(p_i - p_j)]; \quad i \neq j = 1, 2. \tag{8}$$

The formal manipulation of the master equation even in this simplified case is made a little simpler if we introduce the difference in the probabilities

$$\Pi \equiv p_1 - p_2. \tag{9}$$

Subtracting Eq. (2) from Eq. (1) after some algebra yields the highly nonlinear rate equation for the difference variable

$$\frac{d}{dt}\Pi = -(g_{12} + g_{21})\Pi + (g_{21} - g_{12}) \tag{10}$$

where the nonlinearity enters through the transition rate dependence on the difference variable

$$g_{12} = g_0 exp[-K\Pi]; \quad g_{21} = g_0 exp[K\Pi] \tag{11}$$

in the mean field approximation. By inserting Eq. (11) into Eq. (10) we obtain

$$\frac{d}{dt}\Pi = -\frac{\partial V}{\partial \Pi} \tag{12}$$

and the network dynamics are determined by the potential function $V(\Pi)$, which is a symmetric double well potential with the explicit form

$$V(\Pi) = \frac{2g_0}{K}\left[\Pi \sinh K\Pi - \frac{K+1}{K}\cosh K\Pi\right]. \tag{13}$$

The cooperative behavior of the infinitely large ATA coupled network described by Eq. (12) is that of an overdamped particle hopping from one potential minimum to the other, whose position is Π within the potential Eq. (13) as described by Kramers [20]. For $K < 1$, half of the nodes are in the state $|1\rangle$ and half are in the state $|2\rangle$ because there is only a single broad minimum in the potential. At the critical value of the control parameter $K = K_c = 1$ a bifurcation occurs and the potential develops two wells separated by a barrier as discussed by Turalska et al. [35]. The height of the barrier increases with the value of the control parameter.

Professor Werner stressed the importance of criticality in understanding the dynamics of the human brain. A phase transition requires a control parameter, which in physical phenomena is typically the temperature T controlling the density fluctuations in fluids or the magnetic fluctuations in certain solids. At a particular value of the control parameter, the critical value, the qualitative properties of the system change, which is to say there is a phase transition. In the sub-critical region $T < T_c$ the spins in the Ising model [27] are independent of one another and the average magnetization is zero. In the super-critical region $T > T_c$ the spins in the Ising model are strongly coupled and align with one another to yield a non-zero average magnetization. In the critical region $T \approx T_c$ the spins form spatially separated islands, which according to Stanley [33] induces a kind of *short-range order* that is very different from the *long-range order* manifest in the super-critical domain.

It is interesting that at the critical value of the control parameter the ATA version of the DMM undergoes a phase transition. Note that the amplitude of $\xi(t)$ depends on the value of the control parameter K. When $K = 0$, all elements in the network are independent Poisson processes; thereby an average taken at any moment of time over all of them yields zero. Once the value of the coupling becomes nonzero, $K > 0$, single elements are less and less independent,

Please cite this article in press as: West BJ, Turalska M. Network of echoes. Chaos, Solitons & Fractals (2013), http://dx.doi.org/10.1016/j.chaos.2013.06.005

resulting in nonzero averages. The quantity K_c is the critical value of the control parameter K, at which point a phase transition to a global majority state occurs. In numerical calculations we use the time average $\xi_{eq} = \langle|\xi(t)|\rangle$ as a measure of this global majority. More precisely, after an initial 10^6 time steps, the average is taken over the same number of the consecutive time steps of the model. In Fig. 1 the thin line indicates the ATA phase transition as measured by ξ_{eq}. The other phase transitions indicated are for models discussed in the sequel.

Real network are not ATA coupled since interactions typically have finite range and elements are spatially separated. Moreover, real networks have finite numbers of elements. It is therefore useful to examine how strongly the mean field solutions are violated when we relax these constraints. The stability condition can be violated in at least two different ways. The first way is by reducing the number of elements N to a finite value. The second way is by restricting the number of links so the network no longer has ATA coupling. In real networks both sources of equilibrium disruption are expected to occur. For the time being we retain the ATA coupling within the networks and consider the number of elements N to be finite. In this latter case we can no longer make the mean field approximation and the dynamic picture stemming from the above master equation is radically changed.

If the number of elements is still very large, but finite, we consider the mean-field approximation to be nearly valid. The difference variable Π needs to be replaced by the global variable ξ, since the fluctuation frequencies differ from probabilities as $\pi_s^{(\alpha)} = p_s^{(\alpha)} + \varepsilon$. Assuming the independence of noise term ε, one can write the difference variable as $\Pi = p_1 - p_2 + \varepsilon$, and this leads to the transformation of the deterministic equation Eq. (12) into a stochastic differential equation [3,16,35]:

$$\frac{d\xi(t)}{dt} = -\frac{\partial V(\xi)}{\partial \xi} + \varepsilon(t) \tag{14}$$

where the additive fluctuations $\varepsilon(t)$ have amplitudes that are computationally determined to be on the order of $1/\sqrt{N}$. Here again we see the influence of the imperfect imitations that echo between individuals in the network.

Note that the double-well potential in the mean field approximation persists in the present description. The random fluctuations induce transitions between the two states of the potential well. Consequently, for a network with a finite but large number of elements the phase synchronization of Eq. (12) is not stable and the stochastic differential equation represents the dynamics of the network that must be solved. Furthermore the fluctuations can drive the particle from one well of the potential to the other when its amplitude is sufficient to traverse the barrier separating the wells. However, here the fluctuations arise from the finite number of elements in the network rather than from non-existent thermal excitations.

Although Eq. (14) is written in the continuous time representation, in practice the numerical calculations of DMM correspond to the adoption of a finite integration time step $\Delta t = 1$. Note that the stochastic rate Eq. (14) replaces the master equation Eq. (12) in the case of a finite N, and that Eq. (12) is recovered in the ideal case $N = \infty$. Consider the ATA coupling condition with a finite number of elements by numerically integrating the master equation for each element in the network and then calculating the number of elements in each of the two states. In Fig. 2 the fluctuating global variable $\xi(t)$ is depicted as a function of time, under differing conditions. Notice that with increasing N the fluctuation $\xi(t)$ become more distinctly dichotomous-like, with an increasingly sharp transition from the 'up' to the 'down' state. This pattern corresponds to the entire network keeping a decision for a longer and longer time as the size of the network increases. The condition of a decision lasting forever is reached in the ideal case $N = \infty$. The global variable fluctuates between the two minima of the double-well potential as described by Eq. (14) for $K = 1.05 > K_c$ and three values of the size of the network corresponding to an ever increasing influence of the echo network. The single element follows the fluctuations of the global variable, switching back and forth from the condition where the state $|1\rangle$ is preferred statistically to that where the sate $|2\rangle$ is preferred statistically.

Note that if attention were concentrated on a single element in a consensus state that individual would still appear to make transitions according to an exponential distribution. The only measurable difference in the behavior of the individual from that in the non-interacting state would be that she tends to be more reluctant to change her mind. This is a subtle yet profound difference and is a direct result of the imitation mechanism introduced by means of the ERH. Moreover it is reflected in the difference observed between the top and bottom panels of Fig. 2 and may explain why it is so difficult to determine the extent of the influence of group behavior on individual decisions.

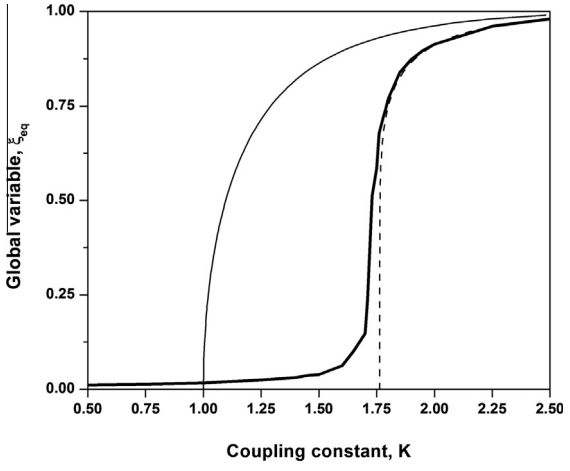

Fig. 1. The phase diagram for the global variable ξ_{eq}. The thin solid line and the dashed line are the theoretical predictions for the fully connected and the two-dimensional regular network, respectively. In both cases $N = \infty$ and the latter case is the Onsager theoretical prediction [27] for a two-dimensional regular lattice. The thick solid line corresponds to the global states observed for the DMM on a two-dimensional regular lattice ($N = 100 \times 100$ nodes) and $g_0 = 0.01$. Periodic boundary conditions were applied in the DMM calculations.

Please cite this article in press as: West BJ, Turalska M. Network of echoes. Chaos, Solitons & Fractals (2013), http://dx.doi.org/10.1016/j.chaos.2013.06.005

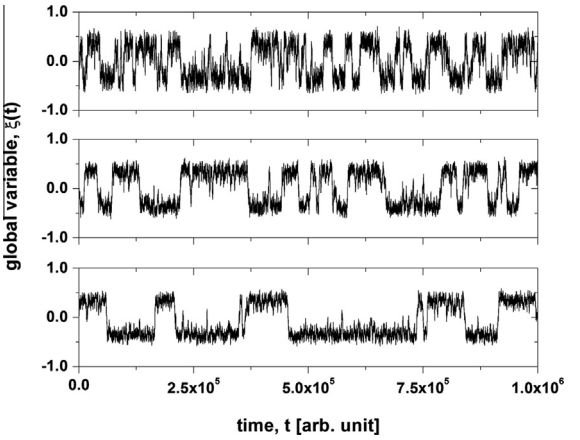

Fig. 2. The fluctuation of the mean field-average phase as a function of time. (top) For a system of $N = 500$ elements, $K = 1.05$ and $g = 0.01$. (middle) For a system of $N = 1500$ elements, $K = 1.05$ and $g = 0.01$. (bottom) For a system of $N = 2500$ elements, $K = 1.05$ and $g = 0.01$.

2.2. Nearest neighbor coupling

Consider a network consisting of N discrete elements located at the nodes of a two-dimensional square lattice. Note that this is a featureless square lattice and the elements are only allowed to directly interact with their nearest neighbors, unlike the ATA coupling network. Each element is a stochastic oscillator whose dynamics are described by s_i that can be found in either of two states $+1$ or -1. The dynamics are introduced by choosing the single element on site i and updating it in an elementary time step using the DMM with a transition rate g_i:

$$g_i(s_i^{+1} \to s_i^{-1}) = g_0 \exp\left[\frac{K}{M}(M_{+1} - M_{-1})\right], \tag{15}$$

$$g_i(s_i^{-1} \to s_i^{+1}) = g_0 \exp\left[\frac{K}{M}(M_{-1} - M_{+1})\right]. \tag{16}$$

Here M denotes the total number of nearest neighbors, which on a square lattice is four, and M_{+1} and M_{-1} are the number of nearest neighbors being in the state $+1$ and -1, respectively. Single elements change states, thereby making the numbers M_{+1} and M_{-1} fluctuate in time, while, of course, the total number of nearest neighbors is conserved, $M_{+1} + M_{-1} = M$.

All numerical calculation in this section are performed on a square lattice of either $N = 50 \times 50$ or $N = 100 \times 100$ nodes with periodic boundary conditions. In a single time step a computer calculation involving the entire lattice is performed and for every element s_i the transition rate of either Eq. (15) or (16) is calculated according to which element is given the possibility to change its state. A single element in isolation is characterized by the control parameter vanishing $K = 0$ and fluctuates between the states with the transition rate $g = g_0$. When the coupling constant is $K > 0$, an element in the state $+1(-1)$ makes a transition to the state $-1(+1)$ faster or slower according to whether $M_{-1} > M_{+1}(M_{+1} > M_{-1})$ or $M_{-1} < M_{+1}$ $(M_{+1} < M_{-1})$, respectively.

Next, we define a global order variable that is completely equivalent to that used in the ATA network:

$$\xi(t) = \frac{1}{N}\sum_{i=1}^{N} s_i. \tag{17}$$

Here again the variability of the global variable does not possess the dichotomous character of single elements. In Fig. 3 we show examples of the temporal evolution for the single element $s_i(t)$. In the upper panel the coupling parameter the time series for a single element is depicted. This signal is not too different from the time series when $K = 0$, but the latter case results in all the elements being independent Poisson processes. In the lower panel the global order variable $\xi(t)$ is depicted for the DMM on a 50×50 two-dimensional lattice with the coupling parameter $K = 1.70$. This value of the control parameter is greater than the ATA critical value, but smaller than the critical value on the lattice.

The solution of the lattice master equation under the assumption of nearest neighbor coupling on an infinite lattice, $M = 4$, $N = \infty$ and $g_0 \to 0$, can be found in [23] and yields the condition for the global variable to be

$$\xi_{eq}(K) = \left(1 - [sinh(K/2)]^{-4}\right)^{1/8}. \tag{18}$$

For this case the critical value of the control parameter is

$$K_c = 2ln\left(1 + \sqrt{2}\right) = 1.7627. \tag{19}$$

Fig. 1 depicts the phase transition under the condition of nearest-neighbor interaction on the two-dimensional lattice and shows that, as expected, the numerical evaluation of $\xi_{eq}(K)$ in the DMM is very close to but less than the theoretical prediction of Onsager [27], thereby confirming that the DMM approaches the Ising model in the limiting case $g_0 \to 0$.

We have interpreted Fig. 1 to mean that when the control parameter K is below its critical value, to the far left in the figure, the elements are statistically independent of one another. When the control parameter is greater than the critical value, to the far right in the figure, the network elements act in concert and cooperative behavior is manifest. So what does this phase transition at the critical value of the control parameter have to do with inverse power laws and topology? The topology of a network describes the connectivity of the elements and had been considered by many investigators to determine a network's dynamics. Consequently, it was also believed that criticality was related to a network's topology. However we have learned that inverse power-law connectivity and criticality are distinct, in part because some scale-free networks do not undergo phase transitions and some critical networks are not scale-free [17,21]. We understand that the transition from essentially independent to cooperative behavior among the elements at the critical point does not occur at all spatial locations of the lattice DMM at the same time. Like the density fluctuations in fluids and the magnetic fluctuations in solids, at the critical point there are islands of correlated fluctuations separated by large regions of uncorrelated variability in the social model. So let us examine this dynamic behavior a little more carefully and determine if this behavior propagates through a social network like a WAVE at a football game or breaks into different parts of the

Please cite this article in press as: West BJ, Turalska M. Network of echoes. Chaos, Solitons & Fractals (2013), http://dx.doi.org/10.1016/j.chaos.2013.06.005

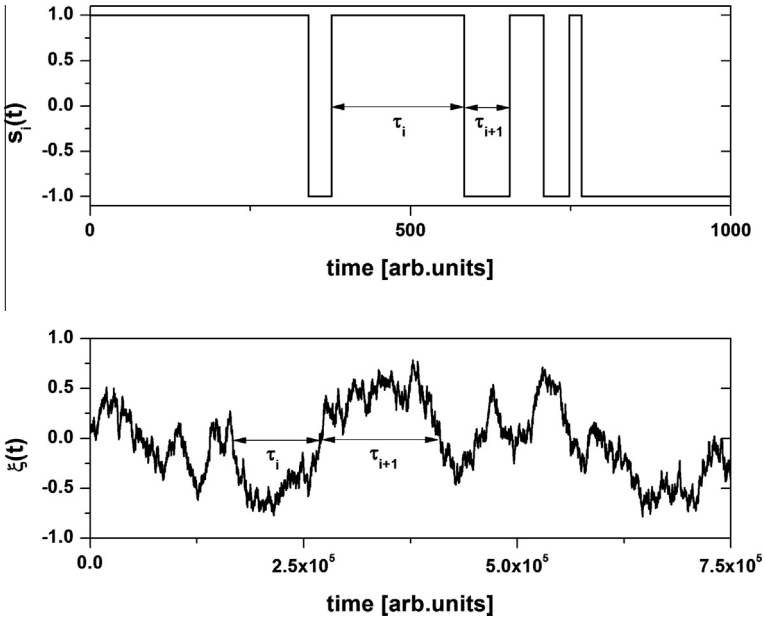

Fig. 3. Temporal evolution of: (Top) a single element $s_i(t)$ and (bottom) of the global order parameter $\xi(t)$; for the DMM realized on a square lattice of $N = 50 \times 50$ nodes, with $g_0 = 0.01$ and $K = 1.70$. To illustrate the concept of crucial events we mark the time intervals τ between two consecutive events, according to their definitions assumed in [36]. Notice the differences in time scales.

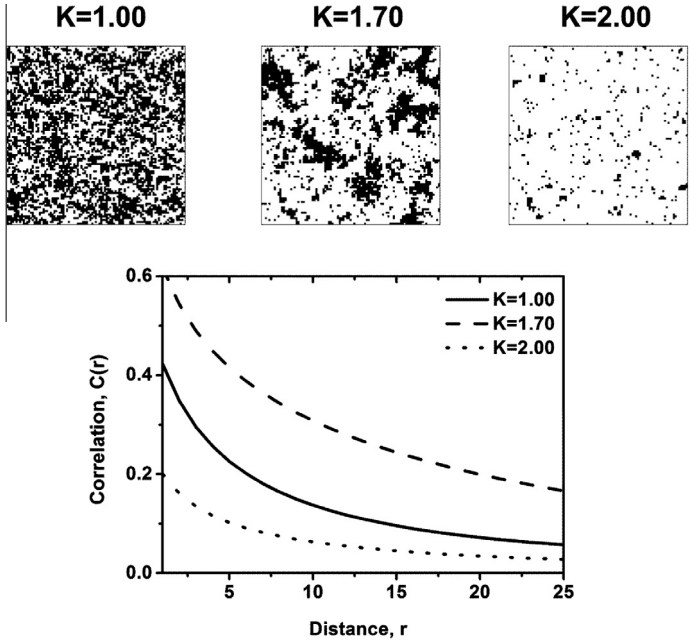

Fig. 4. (Top) The two-dimensional 50×50 lattice over which the DMM elements are distributed. The dynamics is calculated at the three values of the control parameter indicated. White and black indicate the states $+1$ and -1 respectively. (Bottom) Corresponding correlation $C(r)$ as a function of the Euclidean distance r between nodes on the lattice.

network simultaneously, such as the sporadic applause at a child's debut concert.

We display the snapshots of the distribution of opinions across the lattice for three values of the control parameter in Fig. 4. The results are similar to the lattice-gas model results for a fluid system spanning the region of phase transition given in Fig. 1.5 by Stanley [33]. In the left-most panel of the triptych in Fig. 4 the distribution of elements between the up and down states over the lattice is depicted at a point in time for the control parameter $K = 1.0$. Note the control parameter has a value below the critical value on the two-dimensional lattice. The spatially

Please cite this article in press as: West BJ, Turalska M. Network of echoes. Chaos, Solitons & Fractals (2013), http://dx.doi.org/10.1016/j.chaos.2013.06.005

uniform random distribution between the two states is evident. In time this configuration would appear as a flickering background while retaining a lack of coherence. If the signal represented audible sound the room would be filled with static and this static is the echoing of opinions across the lattice.

In the middle panel of the triptych in Fig. 4 is depicted the phase transition region of the two-dimensional lattice with $K = 1.70$. The spatial inhomogeneity of opinion on the lattice is obvious, with like-minded individuals forming clusters that last for a short time and then dissolve. These clusters could be the formation of neighborhoods or political wards that do not break up quickly but persist over time perhaps appearing to crawl over the lattice with a degree of autonomy. Bear in mind that this collective behavior is a consequence of the echo hypothesis and was not part of the dynamic assumptions included in the formation of the lattice DMM.

Finally, in the right-most panel of Fig. 4 the DMM network is shown to have undergone a phase transition with the control parameter above the critical value at $K = 2.0$. The vast majority of individual opinions are in the white state, with a few in the black state being randomly distributed over the lattice. These random points of controversy blink on and off over time, changing their location on the lattice, but for a finite size lattice the overall agreement is never 100%. There are always the few individuals that make life interesting because their opinions are unpredictable.

We use the correlation function $C(r)$ to quantify the arrangement of opinions across the lattice [33]. For values of the control parameter below and above the critical point, the correlation function $C(r)$ decreases rapidly as a function of the distance between nodes. This short-range correlation signifies the discussed lack of cooperation between elements of the lattice. However, close to the critical value of the control parameter, $K = 1.70$, we observe the correlation length to be significantly more extended than in the two other cases. This property, characteristic of systems at a phase transition, arises from collective behavior and tight coupling between distant elements.

The equivalence between a physical phase transition and that of the DMM for a vanishing transition rate is merely formal [36], because the DMM does not have a Hamiltonian origin and does not require an interaction with a thermal bath at temperature T to determine its dynamics. This lack of a temperature in the DMM explains why the equivalence with the Ising model requires that g_0 vanish. The isolated transition rate must vanish in order to freeze the dynamics of the single elements and nullify the ERH.

3. Flavors of complexity

The flavors of complexity addressed in this section are associated with the connectivity of network elements as well as their variability in time. To realize temporal as well as topological complexity we rely on numerical results and focus our attention on the DMM dynamics with $K = 1.70$, which, although slightly smaller than the Onsager theoretical prediction for the critical control parameter, is compatible with the emergence of cooperative behavior due to a phase transition.

3.1. Topological complexity

The dynamically-induced network topology is derived by applying the so-called 'correlation network' approach, where a topology is generated by linking only those elements of a dynamic system whose cross-correlation levels fall above a given threshold [13]. Thus, we record the time evolution of all nodes interacting under DMM dynamics on two-dimensional lattice and we evaluate the linear correlation coefficient between all pairs of nodes. If the cross-correlation coefficient between two nodes is larger than the arbitrarily chosen threshold value Θ, we create a link between them; if not we leave them uncoupled.

This newly created, dynamically-induced topology, called a *Dynamically Generated Complex Topology* (DGCT), clearly depends on the value of coupling used in the DMM dynamics and the threshold Θ applied to the matrix of obtained correlation coefficients. In the subcritical phase, the randomness dominates over the cooperation and results in little correlation between units. Similarly the organized phase is characterized by small values of cross-correlation, which arise from strong coupling between nodes, reducing the variability of each element. However, near the critical point, the coupling between the units is just strong enough to balance the stochasticity. This condition results in much higher values of correlation between nodes that in two previous cases.

The choice of threshold Θ determines the key properties of DGCT topology. In all three dynamic regimes adoption of a low threshold leads to the inclusion of most of the correlation pairs and results in a highly connected network, where almost all nodes are connected to each other. With increasing Θ less and less pairs of nodes are

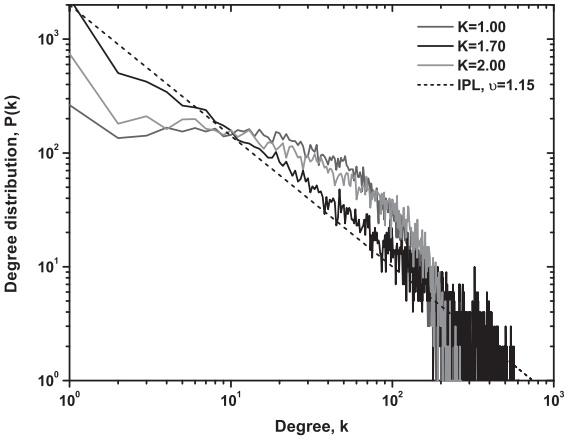

Fig. 5. The degree distribution for the Dynamically Generated Complex Topology created by examining the dynamics of elements placed on a two-dimensional regular lattice with the parameter values $g_0 = 0.01$ and K characterizing three regimes of the DMM behavior. Basic properties of networks characterized by those degree distributions are summarized in Table 1.

correlated highly enough to pass the correlation test and be connected in the new topology. Since for $K < K_C$ and $K > K_C$ the values of correlations are much smaller than those obtained for $K \approx K_C$, the DGCT networks created with the same Θ and increasing K result in different topologies, as shown in Fig. 5. In particular, we find that the correlation network prescription generates a scale-free network with an inverse power index $v \approx 1$ at the value of coupling close to critical one.

The average statistical properties of presented topologies are listed in Table 1. These network's basic properties include the average degree $\langle k \rangle$, average clustering coefficient C, the average path length L and network diameter D [26]. The threshold Θ is adjusted to a value which results in similar $\langle k \rangle$ for three considered regimes of K. Similarly to results reported in [13], the topology constructed from critical DMM dynamics, at $K \approx K_C$, possesses the features of a small world network. It is interesting to observe that the small world property, characterized by high value of the clustering coefficient, is accompanied by an increase in the value of D, suggesting presence of tightly intraconnected subunits, which form the correlation network.

Fig. 6 provides further means of characterizing newly constructed topologies. The plot of average degree $\langle k \rangle$ as a function of correlation threshold Θ illustrates mentioned above fact that with increasing threshold new topology contains fewer connections what results in a smaller $\langle k \rangle$. Additionally, we observe that the network created at $K \approx K_c$ is assortative, as highly connected nodes tend to be connected with equally highly connected neighbors. When comparing with results reported in [13], we note significant similarities in reported properties of topologies based on dynamic correlations. Existing differences we attribute to differences in typical time scale of the DMM and the Ising model and smaller size of the lattice used in DMM calculations.

The DGCT approach is consistent with the procedure widely adopted in neuroscience to define functional connections between different brain regions [13,32]. Numerous studies have shown the scale-free character of networks created by correlated brain activity as measured through electroencephalography [24], magnetoencephalography [31] or magnetic resonance imagining [11]. Fraiman et al. [13] used the Ising model to explain the origin of the scale-free neuronal network, and found the remarkable result that the brain dynamics operate at the corresponding critical state. The present research [35,36] was, in part, inspired by these results [13], and yields the additional discovery that the emergence of consensus produces long-range connections as well as a scale-free topology as a result of the ERH.

Consider the earlier results in the light of the recent experimental findings on brain dynamics [4]. The analysis of Bonifazi et al. [4] established that, in a manner similar to other biological networks, neural networks evolve by gradual change, incrementally increasing their complexity, and rather than growing along the lines of preferential attachment, neurons tend to evolve in a parallel and collective fashion. The function of the neuronal network is eventually determined by the coordinated activity of many elements,

Table 1
Average statistical properties of the DGCT networks.

K	Θ	N	⟨k⟩	C	L	D
1.0	0.45	10,000	50	0.2373	3.3184	8
1.7	0.55	10,000	50	0.5503	4.6963	18
2.0	0.47	10,000	50	0.3532	3.9432	11

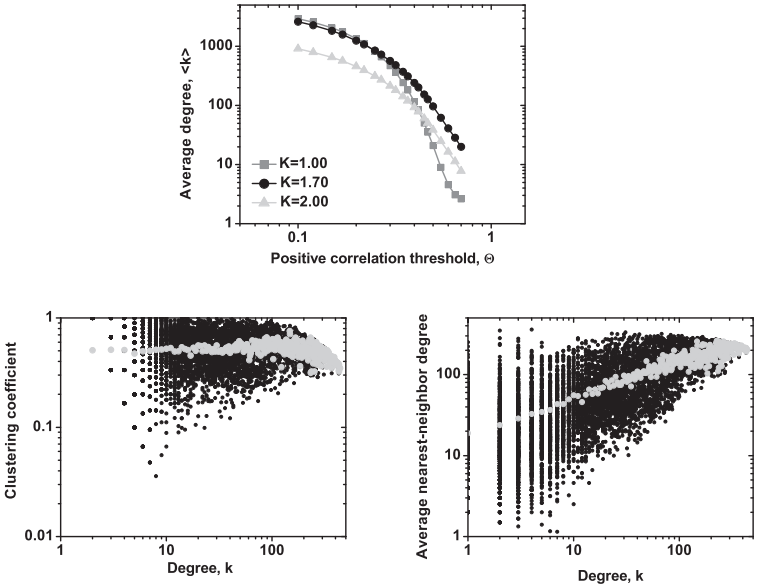

Fig. 6. Average statistical properties of correlation networks. Top: Average degree, $\langle k \rangle$, as a function of threshold Θ for three values of coupling constant K. Bottom right: The average nearest-neighbor degree, $\langle k_{nn} \rangle$, and bottom left: clustering, C, as a function of the degree k for the network extracted from the DMM at K_c. Black dots represent individual nodes and gray ones correspond to averages.

Please cite this article in press as: West BJ, Turalska M. Network of echoes. Chaos, Solitons & Fractals (2013), http://dx.doi.org/10.1016/j.chaos.2013.06.005

with each element contributing only to local, short-range interactions. However, despite this restriction, correlation is observed between sites that are not adjacent to each other, a surprising property suggesting the existence of a previously incomprehensible long-distance communication [8,9]. The DMM dynamical approach along with the ERH affords the explanation that the local but cooperative interactions embed the elements in a phase-transition condition that is compatible with long-range interdependence.

3.2. Temporal distribution

There is a certain amount of arbitrariness in the definition of temporal complexity. But even so we note that the time dynamics of complex networks is characterized by the occurrence of significant events, which may be financial crashes [30], brain quakes [7,13], or the abrupt changes in direction of a flock of birds in flight [5,6]. The time interval between two consecutive critical events is given by a distribution density $\psi(t)$, which, drastically departs from the conventional Poisson statistics, and has the inverse-power-law form

$$\psi(\tau) \propto \tau^{-\mu}, \tag{20}$$

with $\mu < 2$. The occurrence of an event does not have any memory of the occurrence of earlier events. This property is usually denoted as renewal, but it must not be confused with the ordinary Poisson and Markov condition: The signal generated by these critical events is characterized by long-range correlation in time, and, most importantly, it is essentially non-stationary, thereby breaking the ergodicity that is an assumed fundamental property of most models used in statistical physics [29].

The patterns seen in Fig. 4, particularly that at criticality, correspond to the emergence of correlation links yielding a scale-free network statistically indistinguishable from that experimentally observed within the brain, using functional magnetic resonance imaging (fMRI). A number of studies focusing on these patterns emphasize the spatial and network complexity emerging from the cooperative interaction of the network's elements, but overlook the temporal complexity of these networks. We [36] filled this gap by proving that temporal complexity emerges at criticality.

It was established [36] that the apparently intuitive notion that topological complexity with a scale-free distribution in the number of links k, $P(k) \propto k^{-\nu}$ and time complexity with a scale-free distribution in the consensus times τ, are closely related, is not correct. Fig. 7 illustrates the consensus survival probability $\Psi(t)$ corresponding to the critical value of the control parameter $K_c = 1.70$, generating the scale-free topology of Fig. 5. Although emerging from a simple spatial network, that is, from a lattice with no structural complexity, the survival probability is scale-free with $\alpha = \mu - 1 \approx 0.55$ over more than four time decades.

On the other hand, the survival probability of the consensus state emerging from the *ad hoc* network, with $K_c = 1$, and having a scale-free degree distribution is limited to the time region $1/g_0$. In addition for $N \to \infty$ the survival probability in this latter case is expected [35] to be dominated by the exponential shoulder depicted in Fig. 7. The exponential shoulder in the survival probability is a signature of the equilibrium regime of the network dynamics [35] even when the degree distribution retains its scale-free nature.

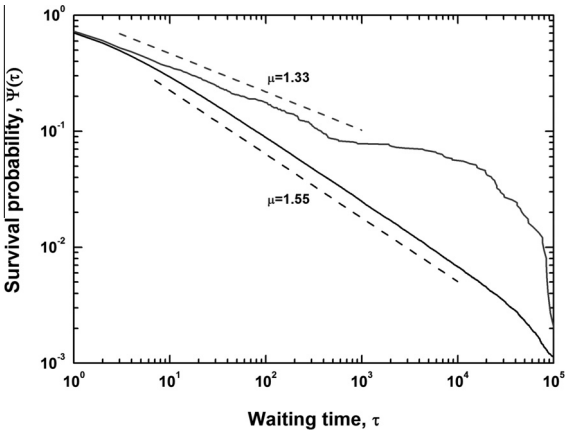

Fig. 7. Consensus survival probability. Black and gray solid lines refer to the DMM implemented on a two-dimensional regular lattice with control paymaster $K = 1.70$ and to dynamics of the *ad hoc* network evaluated for $K = 1.10$, respectively. In both cases $g = 0.01$. The dashed lines are visual guides corresponding to the scaling exponents $\mu = 1.55$ and $\mu = 1.33$, respectively.

4. The mirrored brain

The avalanches recently discovered in neural networks [2] are thought to be manifestations of self-organized criticality [7,28]. The criticality phenomenon has been identified as a plausible model for neural dynamics and is expected to account for the extraordinary long-range interactions between neurons. The cooperation induced at criticality does not imply neural network cognition but Werner [38] advocated that cognition emerges at criticality and its possible relation to extended criticality is taken up by Grigolini et al. [16]. The innovative modeling of the criticality of brain dynamics explaining neuronal avalanches lacked a neurophysiological mechanism even though the mathematical/physical models apparently captured many empirical properties of brain activity. Consequently the closeness of the limiting form of the DMM to the Ising model's phase transition suggests a possible neural mechanism for neuronal avalanches, that being the imitative mechanism contained in the ERH.

We have reviewed how the DMM with imitative interactions among elements manifest critical behavior, including the transition from local independent network elements to global collective interactions in a critical state. In the Introduction the Theory of Imitation was used to motivate the ERH in social networks even though the understanding of the imitation mechanism in the social sciences could not account for collective behavior. The answer to the social scientist's quandary lay in the emergence of criticality due to the nonlinear interaction contained in the implementation of the ERH. However the underlying

mechanism in neural networks must be quite different from that used in social science and another argument for the adoption of ERH in brain dynamics needs to be implemented. To formulate this argument we turn to the recent experimental discovery of mirror neurons.

Historically it had been assumed that neurons in certain areas of the brain preform a sensing function and others perform an action function. As mentioned in the Introduction the nascent discipline of neuroscience was developing at the same time that the theory of imitation was being criticized and investigators were associating various physical locations in the human brain with psychological and behavior function. In 1908 Liepmann [22] determined that the ability to carry out specific actions was lost in patients with lesions in certain areas of the brain. In the past decade the advances in brain imagining due to fMRI has revealed that during imitation tasks a network of regions in the inferior frontal cortex and inferior parietal cortex of the brain are activated [18]. These experiments have called into question the view that neurons perform a single function. Mirror neurons discharge both when a monkey executes an action and when the monkey observes another preforming the same action [25]. Mirror neurons are therefore adaptive imitators that fire when the monkey acts on an object and when the monkey observes another individual making a similar goal-directed action. These neurons show congruence between observed and executed actions.

In the past decade trimodal mirror neurons have been discovered in the monkey ventral premotor cortex; in addition to the motor both visual and auditory function have been observed [19]. In this way it is assumed that the sensing function directly maps the observed activity onto the motor plans necessary to carry out the action, e.g., in the playing of a musical instrument. D'Ausilio [10] emphasizes that "mirror-like mechanisms might be the basis of human music perception-production abilities".

The statistical analysis of the real brain activity led some investigators [14] to conclude that the brain dynamics are dominated by renewal quakes (neuronal avalanches) and that the probability density of the time interval between two consecutive quakes has an inverse power law index $\mu \leqslant 2$. Theoretical arguments [15] establish that this condition is important for the cognitive brain function. On the basis of the plausible conjecture [8] that there is a close connection between the cooperative behavior of many elements and brain cognition, implemented here in the ERH, we believe that the emergence of the condition $\mu < 2$ from the interaction of the elements of the regular two-dimensional lattice, is an important aspect of the dynamic approach to the scale-free condition.

5. Discussion and conclusions

We emphasized that to study the importance of a specific property it is necessary to strip a model down to its simplest form and determine if the emergent property of interest remains. Such simplicity assists us in making the minimal number of assumptions necessary to explain observed behavior. The results presented herein suggest a new mechanism to explain the cooperative behavior seen in flocks, bevies, coveys, gangs and plagues. The new mechanism is embodied in the ERH and entails the generic properties of the DMM. By now it is clear that DMM consists of a network of simple elements that have a decision to make, vote either yes or no, move either right or left, turn either on or off. Left alone each element randomly switches between these two states without bias. However when these individuals are allowed to interact with other members of the network in a way that depends on how many of their colleagues are in one state or the other embodies the ERH and subsequently the overall behavior of the network is dramatically changed.

The echo response mechanism produces a social phase transitions that occurs in both ATA coupling and in nearest neighbor coupling on a lattice. The lattice dynamics are similar to physical critical behavior in a limiting regime, but in general it has a number of significant differences. One particularly significant difference is the cause of the statistical fluctuations, which in physical phenomena is produced by a thermal bath, but in the DMM is the result of the law of large numbers (the finite size of the network).

In neural networks the ERH captures the sensitivity of a given neuron to the dynamics of its neighbors. The phenomenon of criticality imposes on that neuron a sensitivity to the dynamics of the network as a whole. Consequently although a neuron is ostensibly only interacting with its nearest neighbors it responds to the collective activity of the network. In this way an individual comes to a decision and some time later, without any additional information, comes to the totally opposite decision. Without a mechanism to lock the decision in place once it has been made a person will continue to erratically vacillate between alternatives. Does this sound like anyone you know?

References

[1] Baldwin JM. Mental development in the child and the race. New York: Macmillian Company, 1895. Baldwin JM. Social and ethical interpretations in mental development. New York: Macmillian Company, 1897.
[2] Beggs JM, Plenz D. Neuronal avalanches in neocortical circuits. J Neurosci 2003;23:11167–77.
[3] Bianco S, Geneston E, Grigolini P, Ignaccolo M. Renewal aging as emerging property of phase synchronization. Physica A 2008;387:1387.
[4] Bonifazi P, Goldin M, Picardo MA, Jorquera I, Cattani A, Bianconi G, et al. GABAergic hub neurons orchestrate synchrony in developing hippocampal networks. Science 2009;4(5958):1419–24.
[5] Cavagna A, Cimarelli A, Giardina I, Parisi G, Santagati R, Stefanini F, et al. Scale-free correlations in starling flocks. Proc Natl Acad Sci USA 2010;107:11865–70.
[6] Vicsek T, Czirók A, Ben-Jacob E, Cohen I, Shochet O. Novel type of phase transition in a system of self-driven particles. Phys Rev Lett 1995;75:1226–9.
[7] Chialvo DR. Emergent complex neural dynamics. Nat Phys 2010;6:744–50.
[8] Couzin ID. Collective minds. Nature 2007;445:715.
[9] Couzin ID. Collective cognition in animal groups. TRENDS Cogn Sci 2009;13:36–43.
[10] D'Ausilio A. Mirror-like mechanisms and music. Sci World J 2009;9:1415–22.
[11] Eguiluz VM, Chialvo DR, Cecchi GA, Baliki M, Apkarian AV. Scale-free brain functional networks. Phys Rev Lett 2005;94:018102.
[12] Ellwood CA. The theory of imitation in social psychology. Am J Sociol 1901;6:721–41.
[13] Fraiman D, Balenzuela P, Foss J, Chialvo DR. Ising-like dynamics in large-scale functional brain networks. Phys Rev E 2009;79:061922.

Please cite this article in press as: West BJ, Turalska M. Network of echoes. Chaos, Solitons & Fractals (2013), http://dx.doi.org/10.1016/j.chaos.2013.06.005

[14] Gong P, Nikolaev AR, van Leeuwen C. Intermittent dynamics underlying the intrinsic fluctuations of the collective synchronization patterns in electrocortical activity. Phys Rev E 2007;76:011904.
[15] Grigolini P, Aquino G, Bologna M, Luković M, West BJ. A theory of 1/f noise in human cognition. Physica A 2009;388:4192.
[16] Grigolini P, Zare M, Svenkeson A, West BJ. Neural dynamics: criticality, cooperation, avalanches and entrainment between complex networks, Plenz, (ed.), Jon Wiley & Sons, in press.
[17] Haldeman C, Beggs JM. Critical branching captures activity in living neural networks and maximizes the number of metastable states. Phys Rev Lett 2005;94:058101.
[18] Iacoboni M, Woods RP, Brass M, Bekkering H, Mazziotta JC, Rizzolatti G. Cortical mechanisms of human imitation. Science 1999;286:5449.
[19] Kohler E, Deysers C, Umilta MA, Gogassi L, Gallese V, Rizzolatti G. Hearing sounds, understanding actions: action representation in mirror neurons. Science 2002;297:846–8.
[20] Kramers HA. Brownian motion in a field of force and the diffusion model of chemical reactions. Physica 1940;7:284.
[21] Larremore DB, Shew WL, Ott E, Restrepo JG. Effects of network topology, transmission delays and refractoriness on the response of coupled excitable systems to a stochastic stimulus. Chaos 2011;21:025117. http://dx.doi.org/10.1063/1.36007.
[22] Liepmann H. Drei Aufätze aus dem Apraziegebiet. Berlin: Karger Publ.; 1908.
[23] McCoy BM, Wu TT. The Two-Dimensional Ising Model, Cambridge: Harvard University Press; 1973.
[24] Micheloyannis S, Pachou E, Stam CJ, Vourkas M, Erimaki S, Tsirka V. Using graph theoretical analysis of multi channel EEG to evaluate the neural efficiency hypothesis. Neurosci Lett 2006;402:273–7.
[25] Murata A, Fadiga L, Fogassi L, Gallese V, Raos V, Rizzolatti G. Object representation in the ventral premotor cortex (area F5) of the monkey. J Neurophysiol 1997;78:2226–30.
[26] Newman M. Networks: an introduction. New York: Oxford University Press; 2010.
[27] Onsager L. Crystal statistics. I. A two-dimensional model with an order-disorder transition. Phys Rev 1944;65:117–49.
[28] Plenz D. Neuronal avalanches and coherence potentials. Eur Phys J – Spec Top 2012;205:259–301.
[29] Rebenshtok A, Barkai E. J Stat Phys 2008;133:565.
[30] Sornette D. Phys Rep 2003;378:1.
[31] Stam CJ. Functional connectivity patterns of human magnetoencephalographic recordings: a "small-world" network? Neurosci Lett 2004;355:25–8.
[32] Stam CJ, de Bruin EA. Scale-free dynamics of global functional connectivity in the human brain. Hum Brain Mapp 2004;22:97–109.
[33] Stanley HE. Introduction to phase transition and critical phenomena. New York: Oxford University Press; 1971.
[34] Tarde MG. Les Lois de l'Imitation, 1890.Tarde MG. La Logique sociale, 1895.Tarde MG. Les Lois socials, 1898.
[35] Turalska M, Lukovic M, West BJ, Grigolini P. Complexity and synchronization. Phys Rev E 2009;80:021110.
[36] Turalska M, West BJ, Grigolini P. Temporal complexity of the order parameter at the phase transition. Phys Rev E 2011;83:061142.
[37] Turalska M, West BJ, Grigolini P., Role of committed minorities in times of crisis. Scientific Reports 2013;3:1371.
[38] Werner G. Consciousness viewed in the framework of brain phase space dynamics, criticality, and the renormalization group. Chaos Solitons Fract. Special issue. http://dx.doi.org/10.1016/j.chaos.2012.03.014..
[39] Wiener N. Time series. Cambridge, Mass: MIT press; 1949.

Please cite this article in press as: West BJ, Turalska M. Network of echoes. Chaos, Solitons & Fractals (2013), http://dx.doi.org/10.1016/j.chaos.2013.06.005